Correlation between domain wall creep parameters of thin ferromagnetic films

C.P. Quinteros,[1] S. Bustingorry,[1] J. Curiale,[1,2] and M. Granada[1, a)]

[1)] *CNEA, CONICET, Centro Atómico Bariloche, Av. E. Bustillo 9500, (R4802AGP) S. C. de Bariloche, Río Negro, Argentina.*

[2)] *Instituto Balseiro, UNCuyo - CNEA, Av. E. Bustillo 9500, (R4802AGP) S. C. de Bariloche, Río Negro, Argentina.*

(Dated: 1 June 2018)

Designing magnetic materials for potential applications based on domain wall motion requires the knowledge of the relationship between physical properties and phenomenological parameters characterizing domain wall dynamics. We address in this work the study of magnetic-field-driven domain wall motion within the creep regime on a prototypical metallic Pt/Co/Pt stack with perpendicular magnetic anisotropy. By controlling the deposition characteristics, different magnetic properties are achieved, giving rise to different creep parameters. Those phenomenological parameters are found to collapse in a single linear dependence for all samples based on the same material. Moreover, using data in the literature, we show that the same behavior is observed in Au/Co/Au and Tb/Fe based samples. We therefore obtain a pair of global parameters that fully characterize the family of domain wall velocity-field curves within the creep regime for each group of samples, which can be used as input for the optimization of materials.

Keywords: DW motion, creep regime, ferromagnetic films, perpendicular magnetic anisotropy

Magnetic domain wall (DW) motion is expected to play a pivotal role in understanding magnetization reversal dynamics and in the development of magnetic memory devices[1–3]. This has motivated a large number of works from basic research, focusing on understanding the main mechanisms underlying DW motion[4–10], to applications, proposing devices based on DW motion[11–16]. Designing specific materials for applications urges a proper understanding of the relationship between materials properties and DW dynamics[17,18]. In fact, it is desirable for applications to reach a high DW velocity regime at small external drives, thus reducing energy costs. How to reach this high velocity regime, i.e. a fast flow regime where DW velocity is proportional to the external field, strongly depends on the low velocity regimes where DW dynamics is dominated by disorder. A proper understanding of DW dynamics at low drives where disorder dominates, and its relationship with materials parameters, will then serve to design materials for applications based on DW motion.

A direct test of DW dynamics is given by its response to a weak external field, resulting in the thermally activated creep regime. Since the seminal work of Lemerle et al.[4], the creep regime has been deeply investigated[5,9,17,19–22]. In this regime, the DW velocity follows an Arrhenius law of the form

$$v = v_d e^{-\Delta E/(k_B T)}, \tag{1}$$

where ΔE is the effective energy barrier, k_B is the Boltzmann constant, T is the temperature, and v_d is a characteristic velocity at which the DW moves when the energy barrier ΔE vanishes. The effective energy barrier depends on the magnitude of the external field H (see Ref.[10]),

$$\Delta E = k_B T_d \left[\left(\frac{H}{H_d} \right)^{-\mu} - 1 \right], \tag{2}$$

with $k_B T_d$ the characteristic pinning energy scale, H_d the depinning field, corresponding to the underlying zero-temperature depinning transition, and μ is the universal creep exponent ($\mu = 1/4$ for thin ferromagnetic films[4,5,10]). This expression for the velocity-field response has been proven to characterize DW dynamics in a wide field range $0 < H < H_d$ for many different materials[10,18,23]. Noteworthy, the universal DW dynamics depends on three material-dependent parameters: the depinning field H_d, the depinning temperature T_d and the depinning velocity $v_d = v(H_d)$. Having access to these three parameters requires reaching field values beyond the depinning field and gives a full description of both creep and depinning regimes[18,23]. However, small field values can also provide important information about depinning parameters as exemplified by the creep plot $\ln v$ vs. $H^{-1/4}$. This results from rewriting Eqs. (1) and (2) as

$$\ln v = \ln v_0 - \alpha H^{-1/4}, \tag{3}$$

where $\ln v_0 = \ln v_d + T_d/T$ and $\alpha = T_d H_d^{1/4}/T$. The creep plot suggested by Eq. (3) implies that a linear relationship of $\ln v$ vs. $H^{-1/4}$ should be observed below H_d, characterized by a slope α and an intercept $\ln v_0$. Note that v_0 is the depinning velocity v_d multiplied by an exponential of T_d/T, and thus can be considered as a thermal correction to the depinning velocity, while α can be recast as a field $\alpha^4 = H_d(T_d/T)^4$, containing information about the depinning parameters. For example, the dependence of the slope α on materials details and external parameters is commonly used to describe DW

[a)] Electronic mail: granadam@cab.cnea.gov.ar

This manuscript was accepted by Appl. Phys. Lett. Click here to see the version of record.

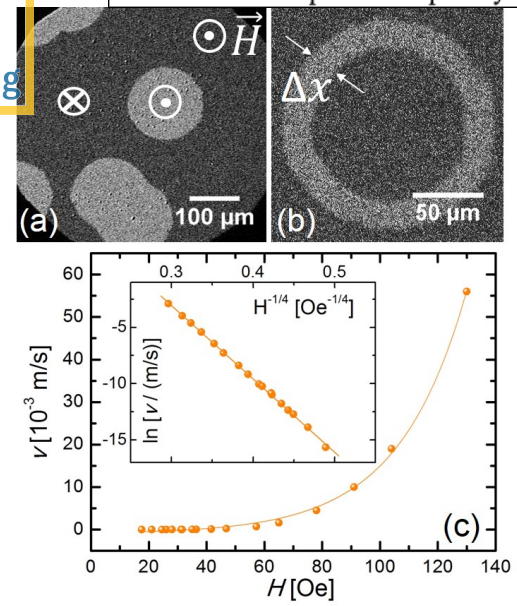

FIG. 1. (a) Typical differential PMOKE microscopy image after nucleation. Two different gray levels indicate the magnetization pointing in opposite directions perpendicular to the sample. (b) Differential image after application of a magnetic field pulse of amplitude $H = 104$ Oe and duration $\Delta t = 1$ ms. (c) Typical $v(H)$ dependence. The inset shows the same result in the usual creep variables, $\ln v$ vs. $H^{-1/4}$. The solid lines are guides to the eyes.

dynamics[17,24–26]. However, although these creep parameters are not enough to define H_d, T_d and v_d, they still contain important information about DW dynamics, giving a first glance of the interplay between disorder, DW elasticity, external field and thermal fluctuations. Establishing strong correlations between creep parameters α and $\ln v_0$ would thus provide a route to better designing materials for future applications.

In this work we studied the correlations between creep parameters from DW velocity measured on Pt/Co/Pt, a prototypical case study for DW motion. We obtain for each studied sample the two creep parameters (slope α and intercept $\ln v_0$) and show that their values for samples with different microscopic characteristics, and thus different magnetic properties, display a linear dependence that was not reported previously. As a main result, we show that the set of parameters describing the linear dependence between $\ln v_0$ and α characterize the whole family of creep plots for a given material.

The studied Pt/Co/Pt films were deposited by DC sputtering on naturally oxidized (001) Si substrates at room temperature. Pt and Co cathodes were sputtered at 20 W and 10 W respectively, in a 3 mTorr Ar atmosphere. The deposition rates were (1.2 ± 0.1) Å/s for platinum and (0.4 ± 0.1) Å/s for cobalt, for a distance from substrate to target of 8.3 cm. The films studied in this work present out-of-plane easy axis of magnetization.

Room temperature magneto-optic Kerr effect magnetometry in the polar configuration (PMOKE) was used to measure out-of-plane magnetization loops, in order to determine the coercive field of the samples. The magnetic field induced DW motion was studied in a home made PMOKE microscope. We work with differential images by subtracting a background image of the fully saturated sample. In Fig. 1(a) a typical differential PMOKE image is shown, where the two different gray levels indicate the magnetization pointing outwards (light gray) and inwards (dark gray) the sample plane. The external magnetic field was applied perpendicular to the sample plane. To measure DW velocity the following protocol was used: first, the magnetization is saturated in a given direction perpendicular to the sample; afterwards, magnetic domains with the magnetization pointing in the opposite direction are nucleated with a short and strong magnetic field pulse; finally, a series of square magnetic field pulses of intensity H and duration Δt are applied and PMOKE images are acquired after each pulse. In Fig. 1(b) a difference between images acquired before and after consecutive field pulses of amplitude H and duration Δt is shown, where the light gray region evidences the domain growth. Domain wall velocity in this case is computed as $v = \Delta x/\Delta t$ with Δx the mean displacement of the DW between successive images. Figure 1(c) shows a typical $v(H)$ curve suggesting a thermally activated law. In the inset, the creep plot $\ln v$ vs. $H^{-1/4}$ is displayed. The observed linear behavior reveals the fact that DW motion takes place in the creep regime, according to Eq (3), and thus is described by the creep parameters $\ln v_0$ and α. In the following, with the aim of studying the effect of microscopic properties on the macroscopic behavior of DWs, i.e. on the creep parameters, we have introduced variations in the deposition details. In particular, we describe the effect of varying the Co thickness and using substrates with different surface topography.

Changes in DW motion produced by modifying the Co thickness are studied in a series of samples Pt(8 nm)/Co(t_{Co})/Pt(4 nm) with $t_{Co} = 0.5$, 0.7 and 0.8 nm. Magnetization loops in Fig. 2(a) show that the coercive field H_C increases with increasing thickness, as observed previously by Metaxas *et al.*[19] and Kim *et al.*[26]. This also agrees with Chowdhury *et al.*[27] who explained that the perpendicular magnetic anisotropy increases monotonically with the magnetic layer thickness up to a limit value above which in-plane anisotropy dominates. The effect of different substrate surfaces on the magnetic properties of Co films, was explored growing the same stack of Pt(8 nm)/Co(0.8 nm)/Pt(4 nm) on (001) Si wafers obtained from different manufacturers, with substrates S1 and S2 corresponding to MTI® and Crystal®, respectively. Room temperature magnetization loops, presented in Fig. 2(b), evidence a large difference between the coercive fields of samples with different substrates. Figures 2(c) and (d) compare DW velocities for samples with different Co thiknesses and for the two samples with different substrates, respectively. It can be observed that the creep plots are different, indicating different creep pa-

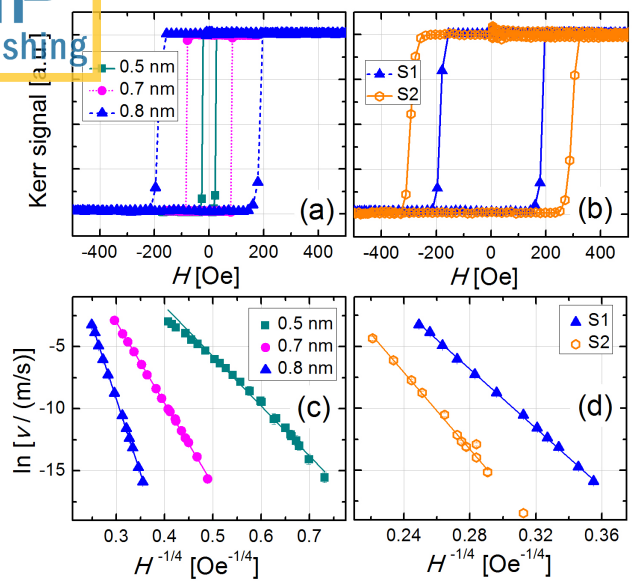

FIG. 2. Magnetization curves measured on (a) Pt(8 nm)/Co(t_{Co})/Pt(4 nm) samples, with t_{Co} = 0.5, 0.7 and 0.8 nm, grown on the same silicon substrate S1, and (b) Pt(8 nm)/Co(0.8 nm)/Pt(4 nm) films grown on (001)Si substrates from different manufacturers, S1 and S2. (c) and (d) display the creep plots, $\ln v$ vs. $H^{-1/4}$, for the same samples as in (a) and (b), respectively. Straight lines in (c) and (d) are linear fits according to Eq. (3).

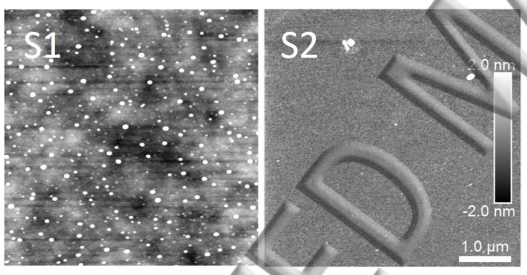

FIG. 3. Atomic force microscopy images for the substrates S1 (left) and S2 (right).

rameters α and $\ln v_0$, according to Eq. (3). On one hand, the results in Fig. 2(c) are consistent with the results presented in Refs. [19,26], where the creep parameters are shown to evolve with the Co thickness and the coercive field. On the other hand, the magnetic properties of equivalent films deposited on S1 and S2 differ from one another even though the substrates are nominally equal, as evidenced by both the coercive field [Fig. 2(b)] and DW velocity-field response [Fig. 2(d)]. This demonstrates that equal Co thicknesses with the same Pt stacks do not assure equal DW dynamics, but also the interfaces with other materials (the substrate in the present case) play a crucial role.

Figure 3 displays atomic force microscopy images of both substrates, where S1 is shown to have higher roughness and density of defects. One can argue that roughness affects the magnetization reversal mechanism and consequently the coercive field. From the energy point of view, a larger coercive field is related to higher potential barriers to be overcome by DWs during the magnetization reversal process. Some authors[28] claim that not only the height of potential barriers but also their distribution could affect magnetization reversal. In particular, the presence of defects such as roughness, bumps, or holes offers additional wells or barriers to the mentioned energetic scenario. In the present case, however, the sample with more defects has a lower coercive field, which suggests that defects are favorable to the domains nucleation process. Furthermore, DW dynamics can also be affected by disorder distribution via its correlation length and energy fluctuations[5,29–31], which can be responsible of the difference observed between the velocity-field curves in Fig. 2(d).

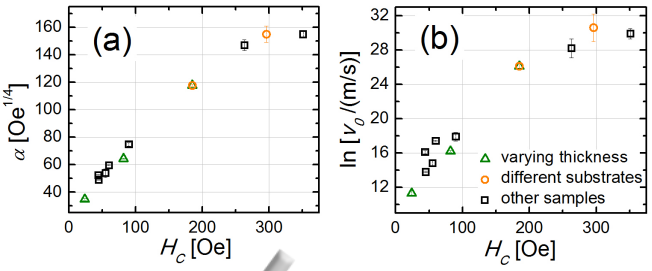

FIG. 4. Creep parameters, (a) slope α and (b) intercept $\ln v_0$ vs. coercive field, obtained from fitting Eq. (3) to $\ln v$ vs. $H^{-1/4}$ curves for different Pt/Co/Pt samples measured in the creep regime. Points corresponding to the curves in Fig. 2 are indicated. Also included are data obtained from samples with different Pt and Co thicknesses grown on different substrates, as discussed in the text.

So far, we have pointed out the effect of magnetic film thickness and substrate topography on the coercive field and DW velocity-field response of the samples. In what follows, we analyze the behavior of the creep parameters obtained from our measurements and then compare with results from other authors. As we have seen in Figs. 2(c) and (d), $\ln v$ vs. $H^{-1/4}$ experimental data follow a linear dependence with well defined creep parameters, slope α and intercept $\ln v_0$, obtained from the linear fit for each sample. In Fig. 4 these creep parameters are plotted as a function of coercive field. We have also included in this figure data for Pt/Co/Pt samples grown with different Co and Pt thicknesses, in the range ±10% with respect to those previously described, and deposited on different substrates (S1, S2, $SrTiO_3$ and SiO_2 thermally grown on S1). Since the coercive field depends on the field sweep rate (Sharrock's law[32]), it is mandatory to compare data with the coercive field measured in equivalent conditions. In this case, PMOKE magnetometry data were acquired while sweeping the magnetic field at 220 Oe/s. Both creep parameters, α and $\ln v_0$, increase with the coercive

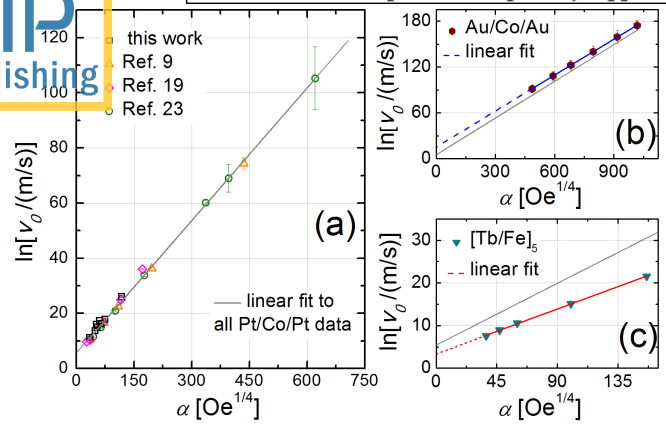

FIG. 5. (a) Creep parameters, intercept $\ln v_0$ vs. slope α for Pt/Co/Pt. Data from this work, presented in Fig. 4, are plotted with black squares. Creep parameters for Pt/Co/Pt samples with different microscopic properties and measured at different temperatures are also included with coloured symbols. Those data correspond to original results presented in Refs. [9[e],19[e],23[e]]. The same plots were constructed for other materials: (b) Au/Co/Au samples from Ref. [33[e]] and (c) [Tb/Fe] multilayers from Ref. [10[e]]. The linear fit from (a) is also displayed as gray lines in (b) and (c) for comparison.

[a] Reproduced with permission from Phys. Rev. Lett. **113**, 027205 (2014). Copyright 2014 American Physical Society.
[b] Reproduced with permission from Phys. Rev. Lett. **99**, 217208 (2007). Copyright 2007 American Physical Society.
[c] Reproduced with permission from Phys. Rev. B **95**, 184434 (2017). Copyright 2017 American Physical Society.
[d] Reproduced with permission from J. Magn. Magn. Mater. **171**, 45 (1997). Copyright 1997 Elsevier Publishing
[e] Reproduced with permission from Phys. Rev. Lett. **117**, 057201 (2016). Copyrght 2016 American Physical Society.

field and seem to display the same dependence on H_C, suggesting a mutual correlation between them.

In order to highlight the strong correlation between creep parameters, in Fig. 5(a) we plot $\ln v_0$ vs. α for all the samples in Fig. 4. Since the coercive field is not relevant for this plot, we have also included results for other Pt/Co/Pt samples with different microscopic properties and measured at different temperatures, already reported in the literature[9,18,19,23]. The creep parameters $\ln v_0$ and α were obtained using $\ln v_0 = \ln v_d + T_d/T$ and $\alpha = T_d H_d^{1/4}/T$ [see Eq. (3)] for values of H_d, T_d and v_d compiled in Ref. [18], corresponding to data originally reported in Refs. [9,19,23] for Pt/Co/Pt thin films. A linear dependence is found to describe all those data. We may now address the question of how universal or material-dependent the curve in Fig. 5(a) is. In order to compare with other materials, we produce the same kind of plot for Au/Co/Au thin films[33] [Fig. 5(b)] and [Tb/Fe] multilayers[10] [Fig. 5(c)]. Again, creep parameters were computed using the data available in Ref. [18] for H_d, T_d and v_d. For the three families of materials presented in Fig. 5 we obtain linear dependencies of the form $\ln v_0 = A\alpha + B$. At this point it is worth noticing that for a given sample one can equate $\ln v_0 = \ln v_d + H_d^{-1/4}\alpha$. However, this does not represent the linear behaviors observed in Fig. 5 since v_d and H_d are sample-dependent parameters. Indeed, the global linear relationship between $\ln v_0$ and α displayed in Fig. 5 is a strong indication of a correlation between the creep parameters of all the samples in the same family. The two global parameters A and B are representative of all the $v(H)$ curves based on the same material, and may differ from one kind of sample to another. Table I sumarizes the parameters obtained from linear fits to the curves in Fig. 5.

Parameter	Pt/Co/Pt	Au/Co/Au	[Tb/Fe]
A (Oe$^{-1/4}$)	0.161 ± 0.001	0.156 ± 0.001	0.12 ± 0.02
B	5.5 ± 0.4	15.9 ± 0.7	3.4 ± 2.0
$H_{\rm cross}$ (Oe)	1488	1689	4823
$v_{\rm cross}$(m/s)	245	8×10^6	30

TABLE I. Fitting parameters A (slope) and B (intercept) for the data in Figs. 5(a), (b) and (c), corresponding to Pt/Co/Pt, Au/Co/Au and Tb/Fe based samples, respectively. Values for $v_{\rm cross}/({\rm m/s}) = e^B$ and $H_{\rm cross} = A^{-4}$ correspond to velocity-field values where the extrapolation of all creep laws converge for a given materials family.

The remarkable fact that all the pairs of $(\alpha, \ln v_0)$ data points lay on the same straight line for a given family of samples, indicates that the parameters A and B characterizing that linear relationship contain valuable information about the DW dynamics for the whole family, regardless of the particular fabrication and measurement conditions. Using that $\ln v_0 = A\alpha + B$, Eq. (3) can be written as $\ln v(H) = B + A\alpha(1 - H^{-1/4}/A) = \ln v_{cross} + H_{cross}^{-1/4}\alpha[1 - (H/H_{cross})^{-1/4}]$, where we have defined $v_{cross}/({\rm m/s}) = e^B$ and $H_{cross} = A^{-4}$. Therefore, from a phenomenological point of view, v_{cross} and H_{cross} would physically correspond to the point where all creep velocity-field curves converge, i.e. $v(H_{cross}) = v_{cross}$. In other words, for example, all Pt/Co/Pt samples would have the same velocity $v_{\rm cross}/({\rm m/s}) = e^B = 245$ at the field $H_{\rm cross} = A^{-4} = 1488$ Oe. The parameters $H_{\rm cross}$ and $v_{\rm cross}$ obtained from A and B are also listed in Table I. The H_{cross} values for all materials are of the same order of magnitude, being somewhat higher for [Tb/Fe]. On the other hand, a large dispersion in v_{cross} values is observed due to the exponential dependence on B. As reported in Ref. [18], values of Td for Au/Co/Au seem to be unusually large, which could be related to a large v_cross. However, further investigation is needed to allow for a detailed discussion on the microscopic origin of v_{cross} and H_{cross}. From a practical perspective, the correlation between creep parameters and coercive field can be used to rapidly estimate DW dynamics for a different sample. For example, if a Pt/Co/Pt sample had a coercive field around 150 Oe, a value of α close to 100 Oe$^{-1/4}$ can be estimated from Fig. 4(a), and using $H_{\rm cross}$ and $v_{\rm cross}$ a value of $\ln v_0 \approx 21.6$ is obtained. With these values for α and $\ln v_0$ the velocity-field curve in the creep regime can be predicted.

As a summary, the impact of Co thickness and substrate topography on DW dynamics was studied in Pt/Co/Pt stacks. Even though the magnetic properties of individual samples (coercive field and DW velocity-field response) are very sensitive to microscopic details, we found that the creep parameters of all Pt/Co/Pt samples can be unexpectedly described by a linear behavior with a pair of global parameters, $H_{\rm cross}$ and $v_{\rm cross}$, which represent the point in the creep plot where all the extrapolated curves for samples of the same materials are crossing. Moreover, using data previously reported in the literature, we found that data for Pt/Co/Pt samples also collapsed on the same linear behavior, independently of the thickness, disorder and temperature of measurement.

This work was supported with grants from ANPCyT (PICT 2013-0014, PICT 2014-2237, PICT 2016-0069), CONICET (PIP11220120100250CO) and UNCuyo (06/C490).

[1] R. L. Stamps, S. Breitkreutz, J. Åkerman, A. V. Chumak, Y. Otani, G. E. W. Bauer, J.-U. Thiele, M. Bowen, S. A. Majetich, M. Kläui, I. L. Prejbeanu, B. Dieny, N. M. Dempsey, and B. Hillebrands, J. Phys. D: Appl. Phys. **47**, 333001 (2014).

[2] F. Hellman, A. Hoffmann, Y. Tserkovnyak, G. S. D. Beach, E. E. Fullerton, C. Leighton, A. H. MacDonald, D. C. Ralph, D. A. Arena, H. A. Dürr, P. Fischer, J. Grollier, J. P. Heremans, T. Jungwirth, A. V. Kimel, B. Koopmans, I. N. Krivorotov, S. J. May, A. K. Petford-Long, J. M. Rondinelli, N. Samarth, I. K. Schuller, A. N. Slavin, M. D. Stiles, O. Tchernyshyov, A. Thiaville, and B. L. Zink, Rev. Mod. Phys. **89**, 025006 (2017).

[3] A. Fert, N. Reyren, and V. Cross, Nat. Rev. Mater. **2**, 17031 (2017).

[4] S. Lemerle, J. Ferré, C. Chappert, V. Mathet, T. Giamarchi, and P. Le Doussal, Phys. Rev. Lett. **80**, 849 (1998).

[5] P. Chauve, T. Giamarchi, and P. Le Doussal, Phys. Rev. B **62**, 6241 (2000).

[6] A. Thiaville, Y. Nakatani, J. Miltat, and Y. Suzuki, Europhys. Lett. **69**, 990 (2005).

[7] S. Bustingorry, A. B. Kolton, and T. Giamarchi, Phys. Rev. B **85**, 214416 (2012).

[8] E. E. Ferrero, S. Bustingorry, and A. B. Kolton, Phys. Rev. E **87**, 032122 (2013).

[9] J. Gorchon, S. Bustingorry, J. Ferré, V. Jeudy, A. B. Kolton, and T. Giamarchi, Phys. Rev. Lett. **113**, 027205 (2014).

[10] V. Jeudy, A. Mougin, S. Bustingorry, W. Savero Torres, J. Gorchon, A. B. Kolton, A. Lemaître, and J.-P. Jamet, Phys. Rev. Lett. **117**, 057201 (2016).

[11] D. A. Allwood, G. Xiong, C. C. Faulkner, D. Atkinson, D. Petit, and R. P. Cowburn, Science **309**, 1688 (2005).

[12] S. S. P. Parkin, M. Hayashi, and L. Thomas, Science **320**, 190 (2008).

[13] M. Hayashi, L. Thomas, R. Moriya, C. Rettner, and S. S. P. Parkin, Science **320**, 209 (2008).

[14] Y. Nii, T. Nakajima, A. Kikkawa, Y. Yamasaki, K. Ohishi, J. Suzuki, Y. Taguchi, T. Arima, Y. Tokura, and Y. Iwasa, Nat. Commun. **6**, 8539 (2015).

[15] Y. Huang, W. Kang, X. Zhang, Y. Zhou, and W. Zhao, Nanotechnology **28**, 08LT02 (2017).

[16] G. Yu, P. Upadhyaya, Q. Shao, H. Wu, G. Yin, X. Li, C. He, W. Jiang, X. Han, P. K. Amiri, and K. L. Wang, Nano Lett. **17**, 261 (2017).

[17] A. W. J. Wells, P. M. Shepley, C. H. Marrows, and T. A. Moore, Phys. Rev. B **95**, 054428 (2017).

[18] V. Jeudy, R. Diaz Pardo, W. Savero Torres, S. Bustingorry, and A. B. Kolton, "Pinning of domain walls in thin ferromagnetic films," (2017), arXiv:1709.08009.

[19] P. J. Metaxas, J. P. Jamet, A. Mougin, M. Cormier, J. Ferré, V. Baltz, B. Rodmacq, B. Dieny, and R. L. Stamps, Phys. Rev. Lett. **99**, 217208 (2007).

[20] S. Emori and G. S. D. Beach, J. Phys. Condens. Matter **24**, 024214 (2012).

[21] K.-W. Moon, D.-H. Kim, S.-C. Yoo, C.-G. Cho, S. Hwang, B. Kahng, B.-C. Min, K.-H. Shin, and S.-B. Choe, Phys. Rev. Lett. **110**, 107203 (2013).

[22] J. Ferré, P. J. Metaxas, A. Mougin, J.-P. Jamet, J. Gorchon, and V. Jeudy, C. R. Physique **14**, 651 (2013).

[23] R. Diaz Pardo, W. Savero Torres, A. B. Kolton, S. Bustingorry, and V. Jeudy, Phys. Rev. B **95**, 184434 (2017).

[24] E. Jué, A. Thiaville, S. Pizzini, J. Miltat, J. Sampaio, L. D. Buda-Prejbeanu, S. Rohart, J. Vogel, M. Bonfim, O. Boulle, S. Auffret, I. M. Miron, and G. Gaudin, Phys. Rev. B **93**, 014403 (2016).

[25] J. P. Pellegren, D. Lau, and V. Sokalski, Phys. Rev. Lett. **119**, 027203 (2017).

[26] D. Y. Kim, M. H. Park, Y. K. Park, J. S. Yu, J. S. Kim, D. H. Kim, B. C. Min, and S. B. Choe, Appl. Phys. Lett. **112**, 062406 (2018).

[27] N. A. Chowdhury and D. Misra, J. Electrochem. Soc. **154**, G30 (2007).

[28] C. Bran, P. Gawronski, I. Lucas, R. P. del Real, P. Strichovanec, A. Asenjo, M. Vazquez, and O. Chubykalo-Fesenko, J. Phys. D: Appl. Phys. **50**, 065003 (2017).

[29] E. Agoritsas, V. Lecomte, and T. Giamarchi, Phys. Rev. E **87**, 042406 (2013).

[30] E. Agoritsas, V. Lecomte, and T. Giamarchi, Phys. Rev. E **87**, 062405 (2013).

[31] N. B. Caballero, E. E. Ferrero, A. B. Kolton, J. Curiale, V. Jeudy, and S. Bustingorry, "Magnetic domain wall creep and depinning: a scalar field model approach," (2018), arXiv:1801.07324.

[32] M. Sharrock and J. McKinney, IEEE Transactions on Magnetics **17**, 3020 (1981).

[33] A. Kirilyuk, J. Ferré, V. Grolier, J. P. Jamet, and D. Renard, J. Magn. Magn. Mater. **171**, 45 (1997).

[34] Data used with permission from: J. Gorchon *et al.*, "Pinning-dependent field-driven domain wall dynamics and thermal scaling in an ultrathin Pt/Co/Pt magnetic film", Phys. Rev. Lett. **113**, 027205 (2014), Copyright 2014 American Physical Society; V. Jeudy *et al.*,"Universal pinning energy barrier for driven domain walls in thin ferromagnetic films", Phys. Rev. Lett. **117**, 057201 (2016), Copyright 2016 American Physical Society; P. Metaxas *et al*, "Creep and flow regimes of magnetic domain-wall motion in ultrathin Pt/Co/Pt films with perpendicular anisotropy", Phys. Rev. Lett. **99**, 217208 (2007), Copyright 2007 American Physical Society; R. Diaz Pardo *et al.*, "Universal depinning transition of domain walls in ultrathin ferromagnets", Phys. Rev. B. **95**, 184434 (2017), Copyright 2017 American Physical Society.; A. Kirilyuk *et al.*, "Magnetization reversal in ultrathin ferromagnetic films with perpendicular anisotropy", J. Magn. Magn. Mater. **171**, 45 (1997), Copyright 1997 Elsevier Science.

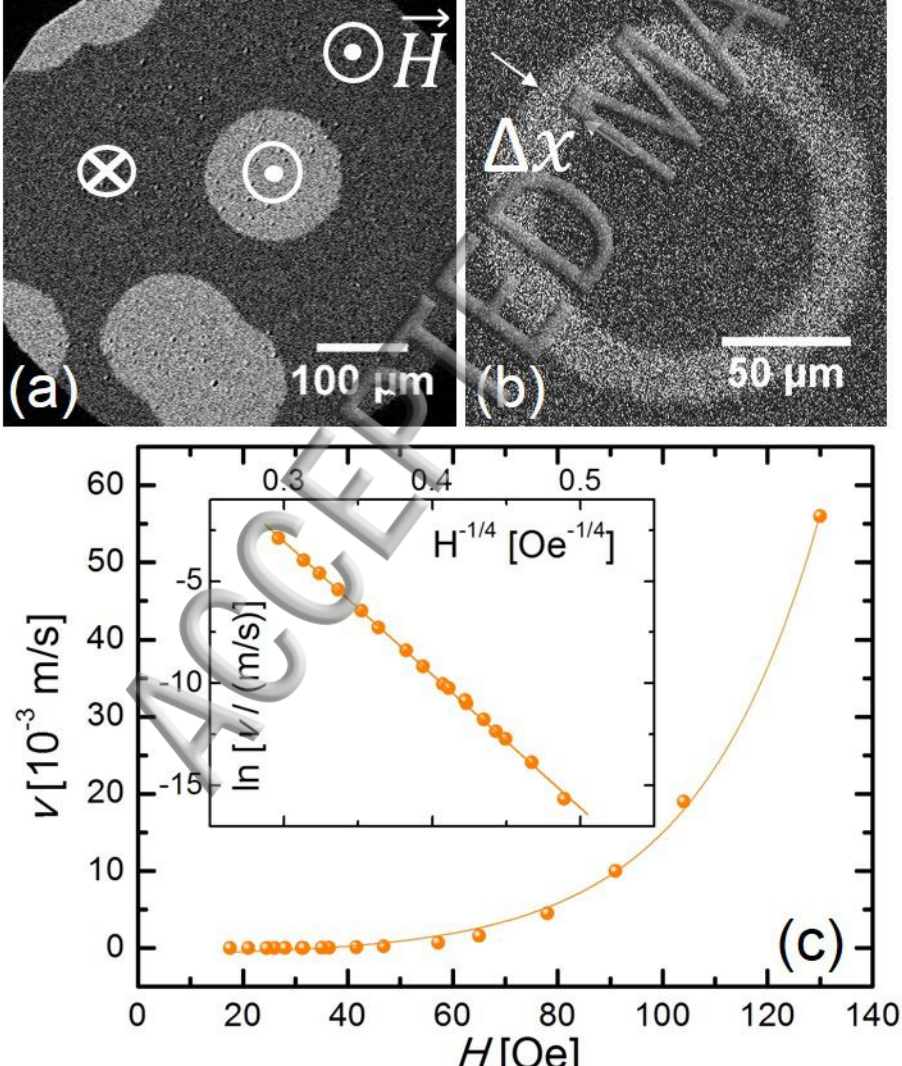
$\vec{H}$
(a)
100 μm
Δx
(b)
50 μm
(c)
v[10^{-3} m/s]
H [Oe]
$H^{-1/4}$ [$Oe^{-1/4}$]
ln [v / (m/s)]

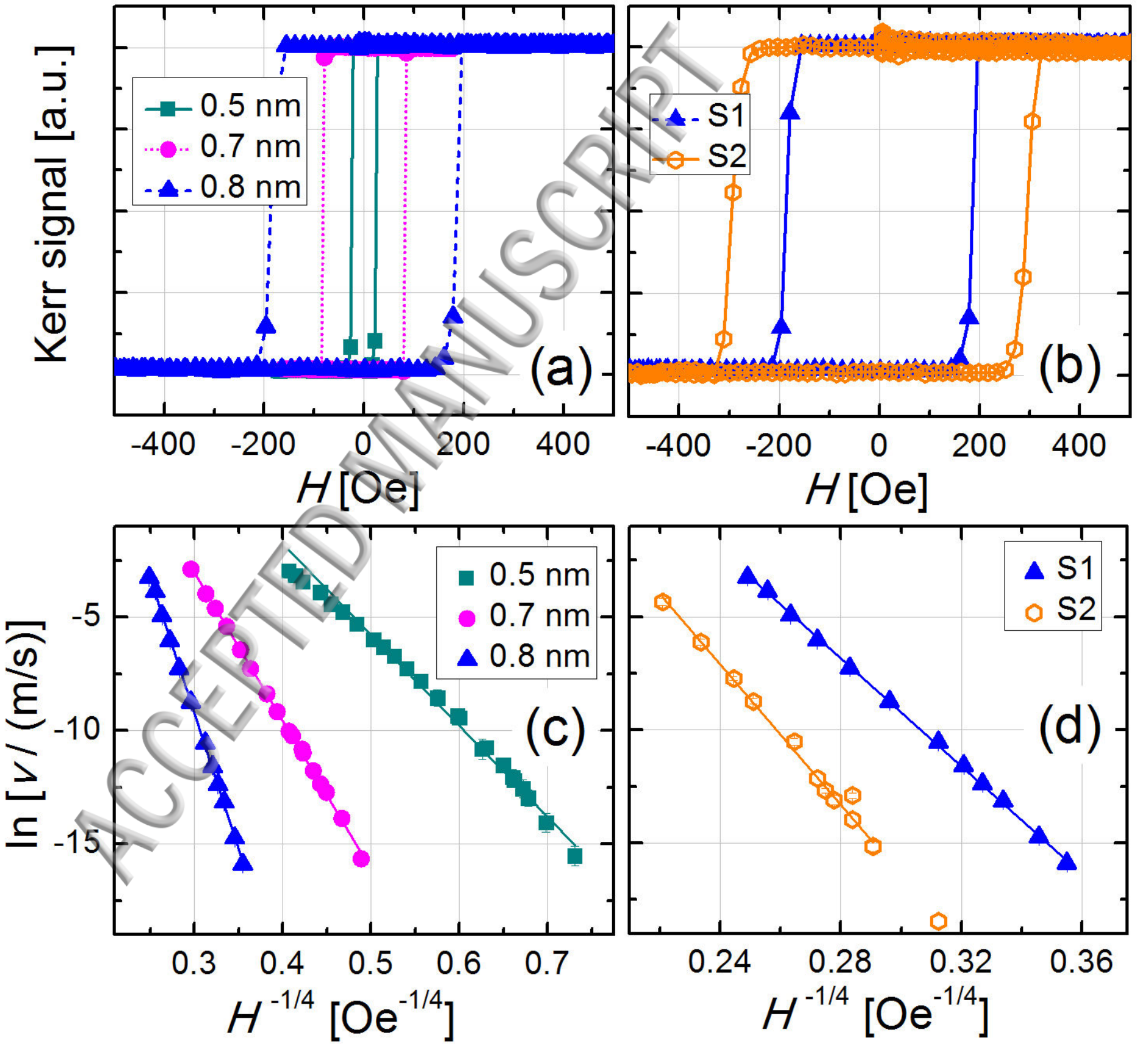

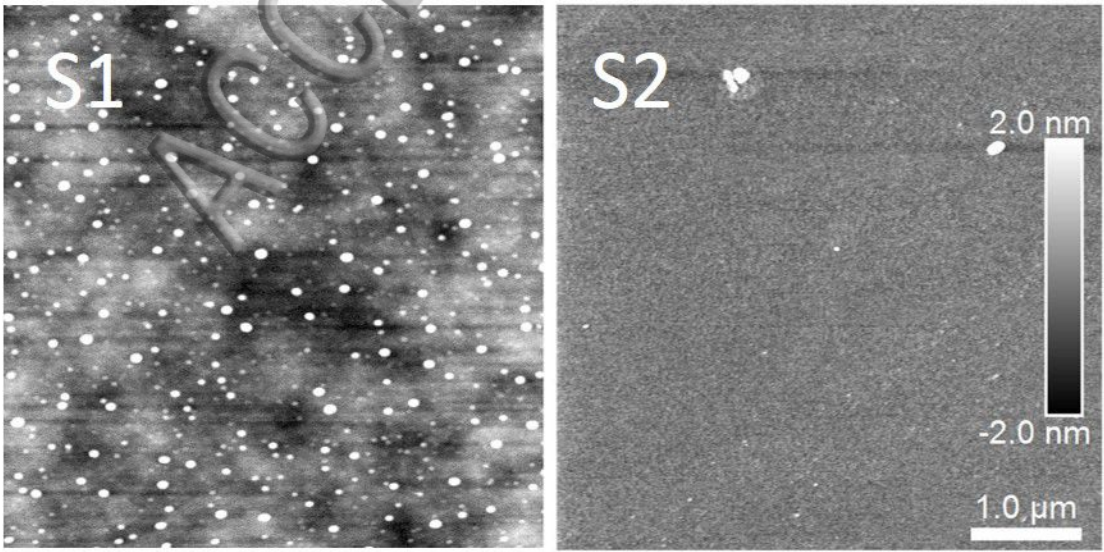
S1
S2
2.0 nm
-2.0 nm
1.0 μm

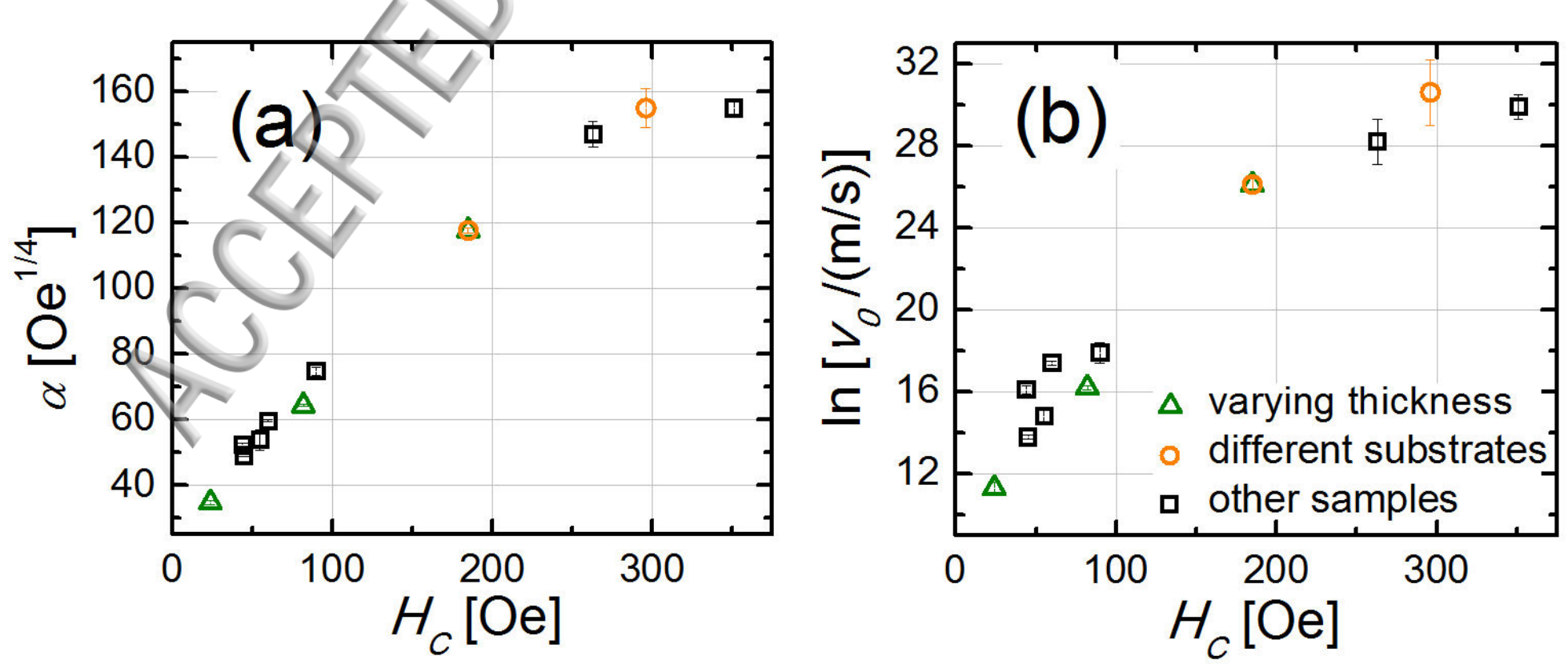
(a)
α [Oe^1/4]
H_c [Oe]
(b)
ln [v_o /(m/s)]
H_c [Oe]
varying thickness
different substrates
other samples